Quantum theory of temporally mismatched homodyne measurements with applications to optical-frequency-comb metrology

Noah Lordi [1,*,†] Eugene J. Tsao [2,3,*,‡] Alexander J. Lind,[2,1,3] Scott A. Diddams,[2,1,3] and Joshua Combes [2]

[1]*Department of Physics, University of Colorado Boulder, 2000 Colorado Avenue, Boulder, Colorado 80309, USA*

[2]*Electrical, Computer, and Energy Engineering, University of Colorado Boulder, 1111 Engineering Drive, Boulder, Colorado 80309, USA*

[3]*Time and Frequency Division, National Institute of Standards and Technology, 325 Broadway, Boulder, Colorado 80305, USA*

The fields of precision timekeeping and spectroscopy increasingly rely on optical-frequency-comb interferometry. However, comb-based measurements are not described by existing quantum theory because they exhibit both large mode mismatch and finite-strength local oscillators. To establish this quantum theory, we derive measurement operators for homodyne detection with arbitrary mode overlap. These operators are a combination of quadrature and intensity-like measurements, which inform a filter that maximizes the quadrature-measurement signal-to-noise ratio. Furthermore, these operators establish a foundation to extend frequency-comb interferometry to a wide range of scenarios, including metrology with nonclassical states of light.

I. INTRODUCTION

Homodyne measurements [1] are foundational to quantum optics and precision metrology, enabling the manipulation [2,3] and characterization [4–6] of quantum states. In a single mode, homodyne measurement is understood as a measurement of a quadrature of the electromagnetic field [7–10]. Many multimode formulations of homodyne measurement assume the signal and local oscillator (LO) share the same temporal mode [11–16], resulting in qualitatively similar quantum descriptions and limits as the single-mode case. Temporal-mode mismatch between the signal and LO has been understood as effective loss [4,5,17–19]. However, these works do not consider the effects of finite-strength LOs, and large mode mismatch evident in many experiments [20–22]. In fact, these experiments observe additional shot noise due to mode mismatch, which is unexplained by effective loss alone.

Over the past two decades, optical frequency combs [23] have emerged as a powerful tool for characterization and dissemination of the most precise clocks [24–26], precision spectroscopy [27,28], and broad bandwidth frequency synthesis [29–31]. In these measurements, the frequency-comb LOs have very high peak power, but relativity small average power; as a result the finite-strength LO effects are important, particularly when the signal has similar average power to the LO. As comb-based measurements near putative shot-noise quantum limits [20,25,32,33], a quantum measurement description that addresses temporal-mode mismatch and finite field strengths is crucial to determine the fundamental bounds on precision. A complete quantum theory also forms the foundation of

frequency comb metrology with nonclassical light [34–37]. We expect this to be important for comb-based measurements aimed at surpassing the standard quantum limit [38–42].

In this article, we address this need by providing a quantum description of temporally mismatched homodyne measurement, shown in Fig. 1. Specifically, we derive the measurement operators, i.e., the positive operator-valued measure (POVM), which enable the calculation of measurement statistics for any signal state and coherent LO both with arbitrary time dependence.

This article is organized as follows. In Sec. II we use continuous mode quantum optics and the Gram-Schmidt procedure to decompose the mode of an incoming signal into the mode of the LO and an orthogonal mode. This temporal-mode decomposition is used to derive measurement operators for modal homodyne measurement in Sec. III, which is our main result. The measurement operator consists of two parts:
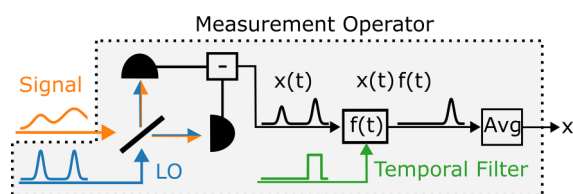

FIG. 1. Temporally mismatched homodyne measurement with signal processing. The signal and local oscillator (LO) have different temporal modes, resulting in a mismatch. The detectors produce a photocurrent proportional to the intensity of the field and the instantaneous difference is denoted by $x(t) \propto I_1(t) - I_2(t)$. We compute the measurement operators for this setup and consider filtering the photocurrent. This filtering removes the additional shot noise due to mode mismatch [20]. We describe the set of filters that do not affect the measured quadrature and achieve signal-to-noise ratios (SNRs) considerably larger than the unfiltered SNR.

---

[*]These authors contributed equally to this work.

[†]noah.lordi@colorado.edu

[‡]eugene.tsao@colorado.edu

a quadrature measurement (corresponding to the LO mode) and an intensity-like measurement (corresponding to the orthogonal mode). We then illustrate our formalism in Sec. IV with several examples. Specifically we use our analysis to develop a new quantum limit for comb-based measurement and provide quantum theoretic grounds for experimental results demonstrating better-than-shot-noise-limited performance by Deschênes and Genest [20] via temporal filtering. We also present measurement statistics for an example nonclassical signal that, to our knowledge, cannot be described by existing analyses. Finally, we conclude in Sec. V with a discussion of the implications of our results for heterodyne measurement, which is the standard measurement with frequency combs.

II. CONTINUOUS MODES AND GRAM-SCHMIDT

In a balanced homodyne measurement, the signal and LO are combined on a beam splitter and both output ports are detected. The resulting photocurrents are then subtracted, and the difference is recorded as the measurement result (see Fig. 1). Typically, the LO strength dominates the signal strength and the LO is temporally mode matched to the signal. Here we do not assume that the signal and LO are mode matched and allow for arbitrary mode overlap. For this reason we need to introduce the basics of continuous mode quantum optics [14].

We begin by defining the mode creation operator $\hat{A}^\dagger(\xi)$ in some temporal mode $\xi(t)$, also known as the field envelope,

$$\hat{A}^\dagger(\xi) = \int_0^T dt\, \xi(t)\hat{a}^\dagger(t), \tag{1}$$

where $\hat{a}^\dagger(t)$ is the creation operator that creates a photon at time t. These mode operators carry the usual commutation relations $[\hat{A}(\xi), \hat{A}^\dagger(\xi)] = 1$ unlike the instantaneous creation operators which have units of $s^{-1/2}$ as can be seen from $[\hat{a}(t), \hat{a}^\dagger(t')] = \delta(t - t')$.

To describe time-dependent homodyne measurements we introduce independent and arbitrary complex temporal modes for the signal and LO, denoted by the mode functions $\xi_S(t)$ and $\xi_{LO}(t)$. These modes are normalized over the detection interval $(0, T)$, i.e., $\int dt' |\xi(t')|^2 = 1$. To analyze this measurement we build an orthonormal basis of temporal modes around the LO mode. This is physically motivated as the time dependence of ξ_{LO} is known and controlled in an experiment.

We construct this basis using the standard Gram-Schmidt process beginning with ξ_{LO} and ξ_S. We label this basis as $\{\xi_{LO}, \xi_\perp, \xi_3, \dots\}$,[1] and define

$$\xi_{LO}(t) = \xi_{LO},$$
$$\xi_\perp(t) = \frac{\xi_S - \langle \xi_{LO}, \xi_S \rangle \xi_{LO}}{\sqrt{1 - |\langle \xi_{LO}, \xi_S \rangle|^2}}, \tag{2}$$

---

[1]The numbered modes are necessary to complete the temporal-mode basis, but will not contribute to the measurement operators. Additionally the above basis is ill defined if $\xi_{LO} \propto \xi_S$, but this is the mode-matched limit where theoretical treatments already exist.
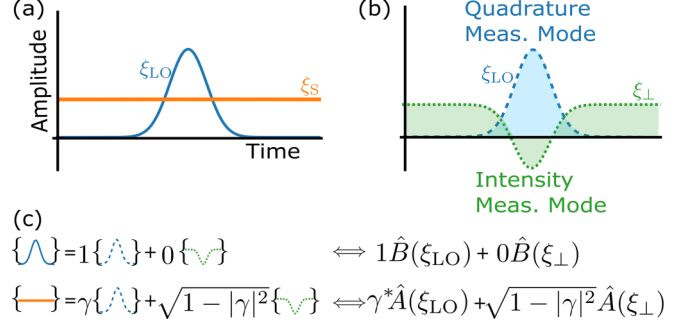

FIG. 2. (a) The physical CW signal (orange) and Comb pulse LO (blue) modes incident on the beam splitter. (b) The Gram-Schmidt modes which correspond to quadrature measurement and intensity-like measurement. (c) The signal and LO modes have some overlap, but we can decompose them into the Gram-Schmidt basis. We can write the signal and LO as a linear combination of these basis elements; here γ is the complex-valued mode overlap, $\gamma = \langle \xi_{LO}, \xi_S \rangle$. This same decomposition can be used on the operators $\hat{B}(\xi_{LO})$ and $\hat{A}(\xi_S)$.

where $\langle f, g \rangle = \int_0^T dt' f^*(t')g(t')$ is the inner product. For convenience we also define the mode overlap, $\gamma \equiv \langle \xi_{LO}, \xi_S \rangle$. The measurement can be completely understood in these two modes because the signal can be decomposed into a linear combination of just ξ_{LO} and $\xi_\perp$.

To demonstrate how to decompose an example signal we can consider the case where the signal is continuous wave (CW) and the LO is a Gaussian pulse, representing, e.g., a short temporal section of a frequency comb. In the frame rotating at the carrier frequency, we have

$$\xi_S = \frac{e^{i\phi}}{\sqrt{T}} \quad \text{and} \quad \xi_{LO} = \left[\frac{e^{-(t-\mu)^2/(2\sigma^2)}}{\sqrt{2\pi\sigma^2}}\right]^{1/2}. \tag{3}$$

Figure 2 illustrates these modes with $\mu = T/2$, $\sigma \approx 0.1T$, and $\phi = 0$. Assuming the LO pulse is fully contained in the detection interval the mode overlap is $\gamma = (8\pi\sigma^2 T^{-2})^{1/4}e^{i\phi}$. The mode overlap is maximized when the ratio of the pulse width to the detection interval is maximal. Intuitively this is when the pulse is the most "CW-like" on the detection interval. Furthermore, the appearance of the phase $e^{i\phi}$ demonstrates that the mode overlap is complex in general.

Using Eq. (2) we can also calculate the perpendicular mode

$$\xi_\perp = \frac{e^{i\phi}}{\sqrt{T - \sigma\sqrt{8\pi}}}(1 - 2e^{-(t-\mu)^2/(4\sigma^2)}), \tag{4}$$

which is pictured in Fig. 2(b). This mode represents the piece of the signal that does not interact with the local oscillator. We will see in Sec. III that the perpendicular mode will contribute intensity-like noise.

Returning to the general case where the modes ξ_S and ξ_{LO} are arbitrary, we define modal coherent states as [14,18,43]

$$|\alpha_{\xi_S}\rangle = D(\alpha, \xi_S)|0\rangle = \exp[\alpha\hat{A}^\dagger(\xi_S) - \alpha^*\hat{A}(\xi_S)]|0\rangle. \tag{5}$$

It is straightforward to show that $A(\xi_S) = \gamma^* A(\xi_{LO}) + \sqrt{1 - |\gamma|^2}A(\xi_\perp)$. Using this along with an application of the Baker-Campbell-Hausdorff formula, and

$[\hat{A}(\xi_1), \hat{A}^\dagger(\xi_2)] = \langle \xi_1, \xi_2 \rangle$, and we get the modal decomposition,

$$
\begin{aligned}
D(\alpha, \xi_S) = {}& D(\gamma \alpha, \xi_{LO}) \otimes D(\sqrt{1-|\gamma|^2}\alpha, \xi_\perp) \\
& \times \exp\left\{ |\alpha|^2 \left(\mathrm{Im}(\gamma^* \sqrt{1-|\gamma|^2} \langle \xi_\perp, \xi_{LO} \rangle) \right) \right\}. \quad (6)
\end{aligned}
$$

Since we have defined our mode basis to be orthonormal we know that $\langle \xi_\perp, \xi_{LO} \rangle = 0$ and thus the exponential term is 1. This allows us to decompose a coherent state signal into the LO and $\perp$ modes:

$$
\left| \alpha_{\xi_S} \right\rangle = \left| \gamma \alpha_{\xi_{LO}} \right\rangle \otimes \left| \sqrt{1-|\gamma|^2} \alpha_{\xi_\perp} \right\rangle. \quad (7)
$$

This will be useful in Sec. IV when we consider the measurement of a coherent signal.

III. MODAL HOMODYNE MEASUREMENTS

The photodetectors in homodyne measurements respond to intensity. In the noiseless limit, intensity detection is photon-number resolving. Like previous work [10,44], we use photon-number-resolving detectors for our analysis, but the noisy detector limit can always be recovered by coarse graining. However, in our analysis, we must consider photodetection in certain temporal modes. That is, we model photodetection as projections onto Fock states in a given mode,

$$
|n_\xi\rangle = \frac{\hat{A}^\dagger(\xi)^n}{\sqrt{n!}} |\mathrm{vac}\rangle, \quad (8)
$$

which are eigenstates of the number operator $\hat{A}^\dagger(\xi)\hat{A}(\xi)$. We use the notation where operators with modes are written in parentheses, $M_{n,m}(\xi)$, and states in modes are denoted with subscripts, $|n_\xi\rangle$.

We assume the detector is unable to differentiate a LO-mode photon from an orthogonal-mode photon. The detector acts as a projector onto a combination of all the possible modes in our basis that could produce a click. For this reason, we construct the n-click measurement operator by marginalizing over the mode degree of freedom,

$$
|\mathrm{vac}\rangle\langle n|_D = \sum_{p=0}^{n} |\mathrm{vac}\rangle (\langle p_{\xi_{LO}}| \otimes \langle n-p_{\xi_\perp}|), \quad (9)
$$

where we assume our detectors absorb photons, hence the projection onto vacuum. Now we follow the analysis of Ref. [44] to arrive at the measurement (Kraus) operator that corresponds to observing n clicks on one detector and m clicks on the other:

$$
M_{n,m} = \langle n|_{D1} \langle m|_{D2} U_{BS} |\psi_{LO}\rangle. \quad (10)
$$

We choose the LO to be a coherent state in ξ_{LO}, $|\psi_{LO}\rangle = |\beta(\xi_{LO})\rangle \otimes |0_{\xi_\perp}\rangle$. We assume our detectors absorb photons so we have used $\langle n|_{D_1}$ as shorthand for $|\mathrm{vac}\rangle\langle n|_{D_1}$. Here the operator $M_{n,m}$ is not given a mode because it pertains to the total clicks over all modes. At the moment these measurement operators are written in terms of n and m, but ultimately we will express the POVM in terms of the difference and sum photocurrent $x \propto n - m$ and $w \propto n + m$, respectively.

We use the definition in Eq. (9) and reorder the tensor product to write the measurement operators in our preferred basis:

$$
\begin{aligned}
M_{n,m} = {}& \sum_{p,q} \underbrace{\langle p_{\xi_{LO}}| \langle q_{\xi_{LO}}|}_{\text{LO modes}} \underbrace{\langle n-p_{\xi_\perp}| \langle m-q_{\xi_\perp}|}_{\perp \text{ modes}} U_{BS} |\psi_{LO}\rangle, \\
= {}& \sum_{p,q} M_{p,q}(\xi_{LO}) \otimes M_{n-p,m-q}(\xi_\perp), \quad (11)
\end{aligned}
$$

where we assume the beam splitter behaves uniformly across modes (Appendix A), although this assumption can be relaxed [45]. Equation (11) shows a decomposition of the measurement operators into two temporal modes:

$$
M_{p,q}(\xi_{LO}) = \langle p_{\xi_{LO}}| \langle q_{\xi_{LO}}| U_{BS} |\beta_{\xi_{LO}}\rangle \quad (12a)
$$

$$
M_{r,s}(\xi_\perp) = \langle r_{\xi_\perp}| \langle s_{\xi_\perp}| U_{BS} |\mathrm{vac}\rangle. \quad (12b)
$$

To obtain our final result for this operator we need to leverage the methods of Refs. [10,44] which involve four steps.

Step 1. We need to perform a change of variables on our operators so they are written in terms of the sum and difference variables. For both modes now we change from the n and m variables to sum and scaled difference variables,

$$
x = \frac{n-m}{\sqrt{2}|\beta|e^{i\theta}} \quad \text{and} \quad w = n+m, \quad (13)
$$

where θ is the phase of the LO. We do this because we want our operators to describe the observed quantities of the measurement, which is the difference photocurrent. In the large-LO limit, we will approximate x as a continuous variable.

Step 2. We construct the POVM from the measurement operators in Eq. (11) as $E = M^\dagger M$ (Appendix B). After a number of approximations we arrive at

$$
E_{x,w} = \sum_{w'} \int dx' E_{x',w'}(\xi_{LO}) \otimes E_{x-x',w-w'}(\xi_\perp), \quad (14)
$$

where $E_{x,w}(\xi_{LO})$ and $E_{x,w}(\xi_\perp)$ are the POVMs for the measurement in each mode. The POVM elements are the operators that give rise to the statistics observed in an experiment.

Step 3. For the analysis of the LO mode we need to assume the LO is large so that we are in the homodyne limit, which entails assuming that $\langle \hat{n}(\xi_{LO})\rangle_S \ll \langle \hat{n}(\xi_{LO})\rangle_{LO}$, i.e., the LO dominates the signal in the LO mode (Appendix C). Thus the difference variable x is quasicontinuous.

Step 4. We marginalize over the sum variable as it is not typically observed in experiments. We can now state our main result, which is the total POVM for a time-dependent LO:

$$
E_x = \sum_w E_{x,w} = \int dx' E_{x'}(\xi_{LO}) \otimes E_{x-x'}(\xi_\perp). \quad (15)
$$

This result is a convolution of a POVM in the LO and perpendicular modes (Appendix D). We absorbed the Jacobian from changing variables into the single-mode POVMs so that both the total and single-mode POVMs sum to identity. In Eq. (15) x on the left-hand side is the difference photocurrent while x' and $x - x' \equiv v$ on the right-hand side are the difference variable contributions from the LO and $\perp$ mode, respectively [cf. Eq. (11)].

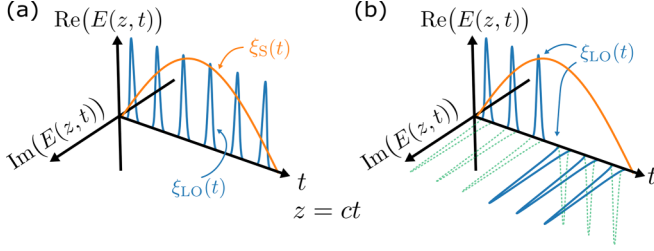A detailed calculation shows the LO-mode POVM is a homodyne measurement of a time-dependent quadrature

FIG. 3. The classical mode functions of a time-dependant homodyne measurement. Here the mode $\xi_{LO}(t)$ is that of a comb, while the signal mode ξ_S is half a period of a sinusoid. (a) The LO phase is constant over the signal and thus the modal quadrature measurement is consistent with a CW quadrature measurement. (b) The phase of the LO has an abrupt change so the time-dependent quadrature is inconsistent with a CW quadrature measurement. Our formalism allows for such time-dependent quadratures. The orthogonal time-dependent quadrature $\hat{P}(\xi_{LO}) = -i(\hat{A}^\dagger(\xi_{LO}) - \hat{A}(\xi_{LO}))/\sqrt{2}$ is the dotted line.

(Appendix B 2)

$$E_{x'}(\xi_{LO}) = |x'_{\xi_{LO}}\rangle\langle x'_{\xi_{LO}}|, \tag{16}$$

where $|x'_{\xi_{LO}}\rangle$ is an eigenstate of the modal quadrature operator $\hat{Q}(\xi_{LO}) = (\hat{A}(\xi_{LO}) + \hat{A}^\dagger(\xi_{LO}))/\sqrt{2}$. This quadrature operator is time dependent in the sense that ξ_{LO} may have different phases at different times (see Fig. 3).

In the perpendicular mode, the LO is in vacuum, and the analysis yields a POVM that follows a binomial distribution in n and m. After switching to sum and difference variables we have (Appendix B 1)

$$E_v(\xi_\perp) = \sum_w |w_{\xi_\perp}\rangle\langle w_{\xi_\perp}| \text{Bin}\left(\frac{|\beta|v}{\sqrt{2}}\Big|w, \frac{1}{2}, 0\right), \tag{17}$$

where $|w_{\xi_\perp}\rangle$ is a Fock state and $\text{Bin}(x|n, p, \mu)$ is a binomial distribution characterized by n and p and shifted so that it has mean μ [46]. Here we have used the difference variable v as if it were discrete, but it must be approximated as continuous to be consistent with Eq. (15). In Eq. (17) the difference variable distribution has mean zero and variance $w/(2|\beta|^2)$, and this is true regardless of the signal state. Only the variance of the difference variable actually depends on the input state. In other words, this is not a quadrature measurement and instead resembles an intensity measurement, as evidenced by the projector onto Fock states.

We have derived the POVM starting from the slow detector limit. For detectors that can resolve the time dependence of the signal and LO the Kraus operators would change. This time-dependent photorecord must be treated carefully. So long as the additional time dependence is averaged over, the measurement statistics predicted by the POVM presented here would remain correct, meaning our POVM is valid in any detector bandwidth limit (Appendix E).

IV. EXAMPLES

We now illustrate the use of these theoretical tools with three examples. We start by considering coherent signals and explore the limits of filtering. In the first two examples, we

apply filtering to a signal with known and unknown temporal profiles. These examples explain a remarkable demonstration by [20] of higher SNR than that set by shot noise of the total photocurrent, achieved by filtering the measurement record. Finally, we utilize our measurement operators to analyze the measurement of a single photon which cannot be calculated using semiclassical methods. Moreover, the filtering technique we explore could be of interest to weak field homodyne measurement when there is mismatch between the weak LO and the signal [47–49].

A. Coherent state signal and SNR bound

We take the signal to be a coherent state $|\psi\rangle_S = |\alpha_{\xi_S}\rangle$ and decompose the signal into the LO mode and the perpendicular ($\perp$) mode as in Eq. (7).

We derive the distribution of the total measurement by taking the expectation of the POVM, Eq. (15), which is $P(x) = \langle\alpha_{\xi_S}|E_x|\alpha_{\xi_S}\rangle$ (Appendix F). If the detector could differentiate photons in the perpendicular and LO modes, then the joint distribution of clicks in the two modes would be

$$P(x_{LO}, x_\perp) = \mathcal{N}(x_{LO}|\mu_{LO}, \sigma_{LO}^2)\mathcal{N}(x_\perp|\mu_\perp, \sigma_\perp^2), \tag{18}$$

where $\mathcal{N}$ denotes a normal distribution, $\mu_{LO} = \sqrt{2}\text{Re}(\alpha\gamma)$, $\sigma_{LO}^2 = 1/2$, $\mu_\perp = 0$, and $\sigma_\perp^2 = |\alpha|^2(1 - |\gamma|^2)/2|\beta|^2$. Here we have used the convention that β is real; i.e., the phase of LO is the reference phase. Because the signal is a coherent state, which is uncorrelated in time, the distributions of $x_\perp$ and x_{LO} are independent. This means if we marginalize, or filter, over the $\perp$ mode we could obtain an "ideal" homodyne measurement of the signal in the LO mode.

The real detectors cannot differentiate between the two modes so the distributions must be convolved, yielding

$$P(x) = \mathcal{N}\left(\mu = \sqrt{2}\text{Re}(\gamma\alpha), \sigma^2 = \frac{1}{2} + \frac{|\alpha|^2(1 - |\gamma|^2)}{2|\beta|^2}\right). \tag{19}$$

From this, we find the power SNR:

$$\text{SNR} = \frac{|\mu|^2}{\sigma^2} = \frac{4|\beta|^2\text{Re}(\gamma\alpha)^2}{|\beta|^2 + (1 - |\gamma|^2)|\alpha|^2}. \tag{20}$$

As the signal and LO become mode matched, i.e., $|\gamma|^2 \to 1$, we recover the expected SNR for ideal homodyne detection: $\text{SNR}_{|\gamma|\to 1} = 4\text{Re}(\gamma\alpha)^2$.

When γ is small and $|\beta|^2 \gg |\gamma\alpha|^2$, i.e., large mode mismatch, a Taylor expansion yields

$$\text{SNR}_{\gamma\to 0}^{\text{total}} \approx \frac{4|\beta|^2\text{Re}(\gamma\alpha)^2}{|\beta|^2 + |\alpha|^2}. \tag{21}$$

Thus $\text{SNR}^{\text{total}}$ has its mean attenuated by the mode-mismatch $\text{Re}(\gamma)$ as predicted by prior theory [4,5,17,19]. Additionally, there are shot-noise contributions from both the signal and LO since no assumption allows either noise term to dominate. The above SNR is conventionally accepted as the quantum limit for frequency-comb measurements [32].

This conventional SNR limit was first questioned in an experiment by Deschênes and Genest [20], where they applied a filter matched to the LO intensity and achieved a sizable SNR improvement over Eq. (21). We reconsider this technique
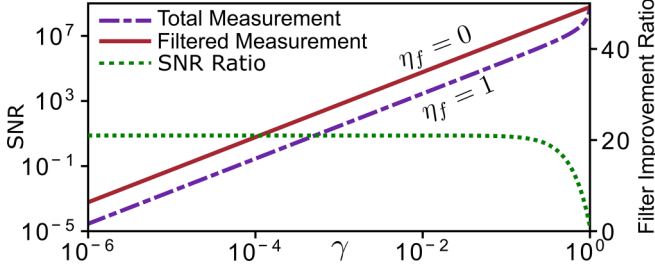
FIG. 4. SNR vs the mode overlap γ with an experimentally relevant set of parameters. The dashed line is the total measurement SNR containing both LO-mode and perpendicular-mode clicks ($\eta_f = 1$). The solid line is the SNR after an optimal filter is applied ($\eta_f = 0$). The dotted line is the improvement obtainable using filtering. For this example we take the signal power to be 2 mW, the LO power is 100 μW, and the measurement interval is $\tau = 10$ ns $= 1/f_{rep}$. For a 10-ps pulse and CW signal we would have typical γ of 10^{-2} and η_f of 10^{-3}; here the available SNR gain is ≈ 13 dB.

specifically for the case where we want to measure the time-dependent quadrature operator $\hat{Q}(\xi_{LO})$ and the mode of the signal ξ_S is unknown.

The optimal filter of the photocurrent is described by the time-dependent weighting function,

$$f(t) = \begin{cases} 1 & \text{if } \xi_{LO}(t) \neq 0 \\ 0 & \text{if } \xi_{LO}(t) = 0, \end{cases} \tag{22}$$

which must be approximated in many cases (Appendix I). This function leaves the LO mode unchanged, so it will preserve the mode of the measured quadrature and leave the mean unchanged. This filter will reduce the shot-noise contribution from the perpendicular mode. The achievable filtered SNR is

$$\text{SNR}^{f(t)} = \frac{4|\beta|^2 \text{Re}(\gamma\alpha)^2}{|\beta|^2 + \eta_f |\alpha|^2}, \tag{23}$$

where η_f is the filtering inefficiency given by $\eta_f = \int dt |f(t)|^2 |\xi_\perp(t)|^2$. When $\eta_f = 0$ (perfect filtering) we recover the ideal homodyne SNR and when $\eta_f = 1$ (no filtering) we have the conventional SNR limit; i.e.,

$$\underbrace{\frac{4|\beta|^2 \text{Re}(\gamma\alpha)^2}{|\beta|^2 + |\alpha|^2}}_{\text{Conventional}} \leqslant \underbrace{\frac{4|\beta|^2 \text{Re}(\gamma\alpha)^2}{|\beta|^2 + \eta_f |\alpha|^2}}_{\text{Achievable}} \leqslant \underbrace{4\text{Re}(\gamma\alpha)^2}_{\text{Ideal}}. \tag{24}$$

We plot these limits for parameter values typical in comb experiments in Fig. 4 and show a 13-dB improvement from perfect filtering. Note that in this derivation, the "comb" structure of the LO is, by definition, included in the mode ξ_{LO} (see Fig. 3), and its impact is described by the overlap with the signal mode ξ_S, i.e., the parameter γ.

We caution that the SNR bounds in Eq. (24) can be beaten if there is prior information about the shape of the signal mode. However, doing so will cause the measurement to no longer be of $\hat{Q}(\xi_{LO})$. For example, if the signal mode is zero while the LO mode is nonzero, that portion of the measurement record only contributes LO shot noise and does not change the mean and could thus be ignored to increase SNR, as explained in Sec. IV B.
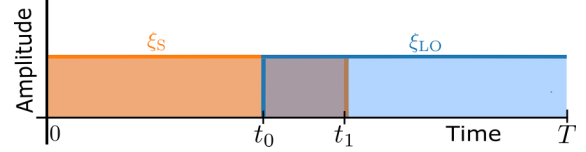

FIG. 5. We show the modes used to demonstrate filtering performance that exceeds our bounds. Here it is clear that the optimal gate would be the one that only counts clicks from the overlapped portion of the measurement and removes all additional shot noise from the LO and signal mode.

B. A known signal mode can violate SNR bound

Now we consider an example where the SNR bounds we proposed can be violated by changing the effective quadrature being measured. We take the signal and LO modes to both be top-hat functions,

$$\xi_S = \begin{cases} \frac{1}{\sqrt{t_1}} & \text{if } t \in (0, t_1) \\ 0 & \text{else,} \end{cases} \quad \xi_{LO} = \begin{cases} \frac{1}{\sqrt{\tau}} & \text{if } t \in (t_0, T) \\ 0 & \text{else,} \end{cases} \tag{25}$$

where $\tau = T - t_0$ (see Fig. 5). The LO defines the modal measurement. As the signal and LO only overlap on the interval (t_0, t_1) we are predominantly measuring vacuum signal.

As the signal mode function is known we may filter out the measurement of vacuum by only considering detection in the interval (t_0, t_1). This is achieved with the filter

$$f(t) = \begin{cases} 1 & \text{if } t \in (t_0, t_1) \\ 0 & \text{else.} \end{cases} \tag{26}$$

This will change the quadrature measured from $\hat{Q}(\xi_{LO})$ to the top-hat "LO mode" in the interval $\hat{Q}(f(t)\xi_{LO})$.

Redoing the above analysis in this case for a coherent signal $|\alpha_{\xi_S}\rangle$, the SNR is

$$\text{SNR} = \frac{4|\beta|^2 \text{Re}(\gamma\alpha)^2}{\eta_{LO}|\beta|^2 + \eta_S |\alpha|^2}, \tag{27}$$

where $\eta_{LO} = (t_1 - t_0)/(T - t_0)$, and $\eta_S = (t_1 - t_0)/t_1$. In the large-LO regime after the filter is applied we get the simplified expression

$$\text{SNR} = \frac{4\text{Re}(\gamma\alpha)^2}{\eta_{LO}}, \tag{28}$$

where we note that η_{LO} is between 0 and 1, so this exceeds the bound we propose of $\text{SNR} = 4\text{Re}(\gamma\alpha)^2$ by a factor of η_{LO}^{-1}. Thus, in this example, because we knew ξ_S, we were able to violate the SNR bound at the cost of altering the modal measurement.

C. Single-photon signal and weak LO

Now consider the signal to be a single-photon state with mode ξ_s. Decomposing this into our basis gives

$$|1_{\xi_s}\rangle = \gamma|1_{\xi_{LO}}\rangle|0_{\xi_\perp}\rangle + \sqrt{1 - |\gamma|^2}|0_{\xi_{LO}}\rangle|1_{\xi_\perp}\rangle. \tag{29}$$

As the overlap between the signal and LO modes increases, the photon is more likely to be found in the LO mode.

To compute the measured quadrature distribution we take the expectation of the POVM in Eq. (15) in the state Eq. (29),
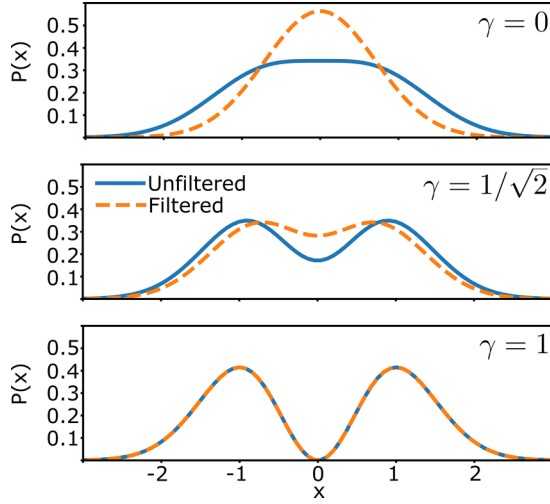
FIG. 6. Difference variable probability distribution for a single-photon signal with varying amounts of mode mismatch. In all figures $\beta = 1$ is used, so that the single photon of shot noise from the signal is not overshadowed. These figures are generated with $\eta_f = 0$. Qualitatively similar results can be observed for larger-photon-number signal states, but combinatorial expansion complicates the analytical formulations equivalent to Eq. (31).

i.e.,

$$P(x) = \int dx' \langle 1_{\xi_s} | E_{x'}^{\text{LO}}(\xi_{\text{LO}}) \otimes E_{x-x'}^{\perp}(\xi_{\perp}) | 1_{\xi_s} \rangle. \quad (30)$$

After some manipulation done in Appendix H, we find

$$P(x) = \frac{1}{2\sqrt{\pi}} \Big[4|\gamma|^2 x^2 e^{-x^2} + (1 - |\gamma|^2)$$

$$\times \left(e^{-(x-1/\sqrt{2}|\beta|)^2} + e^{-(x+1/\sqrt{2}|\beta|)^2} \right) \Big]. \quad (31)$$

The first term is the quadrature distribution for a single photon, which is attained in the mode-matched limit ($\gamma = 1$). For $\gamma = 0$ and $|\beta| \gg 1$ we have the quadrature distribution for vacuum. For γ between these extremes and large β we have the quadrature distribution for a mixed state of zero and one photon. This is the regime that is characterized by an effective loss and is analyzed in detail in Ref. [17]. For small values of β, additional shot noise from the perpendicular mode splits the Gaussian distribution of vacuum into two Gaussians. These features are plotted in Fig. 6. The filtered measurement is equivalent to the effective loss results from Ref. [17], showcasing the difference the added perpendicular mode noise can make. This feature is not present if mode mismatch is treated as just loss and is highly relevant to applications of homodyne measurement with weak LOs [47–49].

V. CONCLUSION

In conclusion, we have found the measurement operators for multimode homodyne detection that are valid for arbitrary time dependence of both the LO and signal. In our construction, the measurement decomposes naturally into two parts: a quadrature measurement in the temporal mode of the LO and an intensity-like measurement on the other modes. We show that perfect filtering of this intensity noise achieves a

quadrature noise-limited measurement. In comb-based measurements characterized by large mode mismatch and strong signals, this establishes a significantly lower quantum limit than conventionally considered. This limit should be sought before pursuing quantum advantage from nonclassical states of light. Moreover, because we have developed a fully quantum theory, we can analyze the measurement of any signal state including squeezed states, which are highly relevant to measurements aimed at increased precision. As an example of our fully quantum theory, we analyzed the measurement of a single-photon Fock state with a finite-strength LO and arbitrary mode overlap. This represents a scenario that existing methods have not been able to fully describe. Our analysis complements related work on POVMs for electro-optic sampling [50].

Many comb-based measurements are based on heterodyne rather than homodyne techniques. Although there are many reasons to prefer homodyne over heterodyne techniques for quantum metrology, the technical limitations of frequency-comb measurements make quantum-limited homodyne measurement more difficult to achieve than heterodyne measurement. We conjecture that the heterodyne SNR is simply half that of homodyne due to sampling of both $\hat{x}$ and $\hat{p}$ quadratures, but a complete analysis of the heterodyne measurement operators is left as future work.

APPENDIX A: MODE DECOMPOSITION OF BEAM SPLITTER

We show that the beam splitter acts the same for every mode, under the assumption that the transmission and reflection coefficients of the beam splitter are constants over the relevant frequencies of the signal and LO mode. From our assumption we have that the action of the beam splitter in every mode is described by the following input-output relations:

$$U_{\text{BS}}^{\dagger}(\xi) \hat{A}(\xi) U_{\text{BS}}(\xi) = \frac{\hat{A}(\xi) + \hat{B}(\xi)}{\sqrt{2}}, \quad (A1a)$$

$$U_{\text{BS}}^{\dagger}(\xi) \hat{B}(\xi) U_{\text{BS}}(\xi) = \frac{\hat{A}(\xi) - \hat{B}(\xi)}{\sqrt{2}}. \quad (A1b)$$

We want to show that this implies a tensor product structure to the beam splitter unitary; i.e., we can split the unitary into a beam splitter for each mode independently. We can demonstrate this by considering decomposing a single mode into a combination of modes and seeing how the unitary must act. Consider an annihilation operator in some mode $\hat{A}(\xi)$. Furthermore, allow ξ to be decomposed as $\xi = c_1 \xi_1 + c_2 \xi_2 +$

$\cdots$. When we conjugate $\hat{A}(\xi)$ by the beam splitter, we have

$$U_{\mathrm{BS}}^{\dagger}\hat{A}(\xi)U_{\mathrm{BS}} = U_{\mathrm{BS}}^{\dagger}\left(\sum_n c_n\hat{A}(\xi_n)\right)U_{\mathrm{BS}}, \tag{A2}$$

but from Eq. (A1) we know this must produce a sum of operators in the ξ mode:

$$U_{\mathrm{BS}}^{\dagger}\left(\sum_n c_n\hat{A}(\xi_n)\right)U_{\mathrm{BS}} = \frac{1}{\sqrt{2}}\sum_n c_n(\hat{A}(\xi_n) + \hat{B}(\xi_n)). \tag{A3}$$

In order for this to hold we need the following to be true:

$$U_{\mathrm{BS}}^{\dagger}\hat{A}(\xi_n)U_{\mathrm{BS}} = \frac{\hat{A}(\xi_n) + \hat{B}(\xi_n)}{\sqrt{2}}. \tag{A4}$$

This equation allows us to write $U_{\mathrm{BS}}(\xi)$ by its action on every mode. This means we can decompose the beam-splitter unitary into modes as

$$U_{\mathrm{BS}} = U_{\mathrm{BS}}(\xi_1) \otimes U_{\mathrm{BS}}(\xi_2) \otimes \cdots, \tag{A5}$$

as desired.

APPENDIX B: DERIVING THE SINGLE-MODE POVMs FROM KRAUS OPERATORS

1. Perpendicular mode

First we address the perpendicular mode, which is significantly easier. We start with Eq. (12b),

$$M_{r,s}(\xi_\perp) = \langle r_{\xi_\perp}|\langle s_{\xi_\perp}|U_{\mathrm{BS}}|\mathrm{vac}\rangle, \tag{B1}$$

which represents r and s clicks in the perpendicular mode. Using the definition of photon number states from Eq. (8) to expand the bras into operators acting in vacuum,

$$M_{r,s}(\xi_\perp) = \langle\mathrm{vac}|\langle\mathrm{vac}|\frac{\hat{A}^r\hat{B}^s}{\sqrt{r!s!}}U_{\mathrm{BS}}|\mathrm{vac}\rangle. \tag{B2}$$

We have omitted the mode label since every operator in this equation acts on the perpendicular mode. We now insert identity, i.e., $U_{\mathrm{BS}}^{\dagger}U_{\mathrm{BS}} = I$, after every operator so we can apply the input-output relations of the beam splitter, $U_{\mathrm{BS}}^{\dagger}\hat{A}U_{\mathrm{BS}} = (\hat{A} + \hat{B})/\sqrt{2}$ and $U_{\mathrm{BS}}^{\dagger}\hat{B}U_{\mathrm{BS}} = (\hat{A} - \hat{B})/\sqrt{2}$. Doing this and applying the remaining beam-splitter unitary to the vacuum modes on the left, we get the following equation:

$$M_{r,s}(\xi_\perp) = \langle\mathrm{vac}|\langle\mathrm{vac}|\frac{(\hat{A} + \hat{B})^r(\hat{A} - \hat{B})^s}{\sqrt{r!s!}2^{(r+s)/2}}|\mathrm{vac}\rangle, \tag{B3}$$

where the $\hat{B}$ operator acts on the Hilbert space of the LO, which in this case is in vacuum. We can apply this vacuum state effectively replacing each $\hat{B}$ operator with a 0 and we get

$$\begin{aligned} M_{r,s}(\xi_\perp) &= \langle\mathrm{vac}|\frac{\hat{A}^{r+s}}{\sqrt{r!s!}2^{(r+s)/2}} \\ &= \langle r + s|\frac{\sqrt{(r+s)!}}{\sqrt{r!s!}2^{(r+s)/2}} \\ &= \langle r + s|\frac{1}{2^{(r+s)/2}}\sqrt{\binom{r+s}{r}}. \end{aligned} \tag{B4}$$

Now we move to the POVMs $E_{r,s} = M_{r,s}^{\dagger}M_{r,s}$,

$$E_{r,s} = \frac{|r + s\rangle\langle r + s|}{2^{(r+s)}}\binom{r+s}{r}, \tag{B5}$$

and change to sum and difference variables as follows:

$$E_{x,w} = \frac{|w\rangle\langle w|}{2^w}\binom{w}{\frac{x}{2} + \frac{w}{2}}. \tag{B6}$$

This is a shifted binomial distribution in x with mean zero in the difference variable and variance w. While we could further approximate this distribution in the limit where w is large we choose not to for two reasons. First, we want the mode-matched limit $\gamma = 1$ to appear naturally from our results and in that limit w in the perpendicular mode goes to zero. Second, the binomial distribution has some nice properties, particularly when coupled with the Poisson distribution of a coherent input state, that make the marginalization integrals analytically solvable. For these reasons we will scale the difference variable, but leave it discrete at the POVM level. Depending on the input state the difference variable can be made continuous in a variety of ways, most commonly by approximating the binomial distribution as normal. The resulting marginalization over w will be difficult under this approximation but can easily be solved numerically. After appropriately scaling variables we get the following POVM:

$$E_{x,w}dx = dx|w\rangle\langle w|\mathrm{Bin}\left(\frac{|\beta|x}{\sqrt{2}}\Big|w, \frac{1}{2}, 0\right), \tag{B7}$$

where $\mathrm{Bin}(x|n, p, \mu)$ is a binomial distribution characterized by n and p and shifted so that it has mean μ:

$$\mathrm{Bin}(x|n, p, \mu) = \binom{n}{x + \frac{n}{2} - \mu}p^{n/2+x-\mu}(1 - p)^{n/2-x+\mu}. \tag{B8}$$

2. LO mode

The calculation in the LO mode is more involved, but has been described in detail in Ref. [44]. We start with Eq. (12a),

$$M_{p,q}(\xi_{\mathrm{LO}}) = \langle p_{\xi_{\mathrm{LO}}}|\langle q_{\xi_{\mathrm{LO}}}|U_{\mathrm{BS}}|\beta_{\xi_{\mathrm{LO}}}\rangle. \tag{B9}$$

We apply the same steps as before up to Eq. (B3), the only difference being that the state of the LO is no longer vacuum. Doing this yields

$$M_{p,q} = \langle\mathrm{vac}|\langle\mathrm{vac}|\frac{(\hat{A} + \hat{B})^p(\hat{A} - \hat{B})^q}{\sqrt{p!q!}2^{(p+q)/2}}|\beta\rangle, \tag{B10}$$

where the mode designations are omitted because every operator and state is in the LO mode. After acting operators on the LO coherent state we arrive at

$$M_{p,q} = \langle\mathrm{vac}|\frac{(\hat{A} + \beta)^p(\hat{A} - \beta)^q}{\sqrt{p!q!}2^{(p+q)/2}}e^{-|\beta|^2/2}. \tag{B11}$$

Now this operator acts only on the signal Hilbert space.

From here we apply a series of algebraic manipulations to arrange the operator into a form where we can apply the large-local-oscillator assumption. When we do this we will assume without loss of generality that $p \geqslant q$, but the calculation goes much the same with the opposite assumption. After

manipulation we get

$$
M_{p,q} = \langle \mathrm{vac}|(-1)^q \left(1 + \frac{\hat{A}}{\beta}\right)^{p-q} \left(1 - \frac{\hat{A}^2}{\beta^2}\right)^q
$$

$$
\times \frac{e^{-|\beta|^2/4}}{\sqrt{p!}} \left(\frac{\beta}{\sqrt{2}}\right)^p \frac{e^{-|\beta|^2/4}}{\sqrt{q!}} \left(\frac{\beta}{\sqrt{2}}\right)^q. \tag{B12}
$$

We have arranged these terms so that we see the appearance of two Poisson distributions in p and q as well as two terms that can be expanded in the large-β limit into exponentials. From here we again move partially to the sum and difference variables of Eq. (13) and also replace m with its mean $|\beta|^2/2$. Applying the large-LO limit allows us to approximate these Poisson distributions as normal as well. Doing this will move us from discrete variables p and q to continuous variables p' and q'. Applying all of these leads us to

$$
M_{p',q'} \approx \langle \mathrm{vac}|(-1)^{q'} e^{\sqrt{2} e^{-i\theta} x \hat{A}} e^{-e^{-2i\theta} \hat{A}^2/2}
$$

$$
\times \left(\frac{e^{-(p'-|\beta|^2/2)^2/(2|\beta|^2)}}{(\pi|\beta|^2)^{1/4}}\right) \left(\frac{e^{-(q'-|\beta|^2/2)^2/(2|\beta|^2)}}{(\pi|\beta|^2)^{1/4}}\right),
$$

$$
\tag{B13}
$$

where $e^{i\theta}$ is the phase of β. Here we recognize the form of a quadrature eigenstate and we combine the two normal distributions to get the much simpler form,

$$
M_{p',q'} = \langle x_\theta| \frac{(-1)^q e^{i\theta(p'+q')}}{|\beta|(\pi)^{1/4}} e^{-(p'+q'-|\beta|^2)^2/(4|\beta|^2)}. \tag{B14}
$$

Now we see that p' and q' only appear in terms of the sum and difference variables so we can completely move to those variables; including the Jacobian terms, we get

$$
M_{x,w} \sqrt{dx\,dw} = \langle x_\theta| e^{iw\theta} (-1)^{q'} \frac{e^{-(w-|\beta|^2)^2/(4|\beta|^2)}}{(2\pi)^{1/4} \sqrt{|\beta|}} \sqrt{dx\,dw}. \tag{B15}
$$

Now we move to the POVMs where the phase terms will cancel, yielding a very simple form

$$
dx\,dw\,E_{x,w} = \frac{e^{-(w-|\beta|^2)^2/(2|\beta|^2)}}{\sqrt{(2\pi)|\beta|^2}} |x_\theta\rangle\langle x_\theta| dx\,dw, \tag{B16}
$$

where we can see that after marginalizing over w we would get

$$
E_x = |x_\theta\rangle\langle x_\theta|, \tag{B17}
$$

as expected.

APPENDIX C: PHOTON-NUMBER CONSIDERATIONS

When discussing the large-LO limit we can break the signal photons into the two modes and compare the number of signal photons that fall into the LO mode to the total number of photons from the LO. There is a subtlety here because we are effectively saying that $\langle\psi_S|\hat{n}(\xi_S)|\psi_S\rangle = \langle\psi_{\xi_{LO}}|\hat{n}(\xi_{LO})|\psi_{\xi_{LO}}\rangle + \langle\psi_{\xi_\perp}|\hat{n}(\xi_\perp)|\psi_{\xi_\perp}\rangle$, which is surprisingly nontrivial, because as an operator equation $\hat{n}(\xi_S) \neq \hat{n}(\xi_{LO}) + \hat{n}(\xi_\perp)$. We know that the first equation must be true because it says that the total number of photons in the signal is equal to

the number of photons from the signal in the LO mode plus the number of photons from the signal in the perpendicular mode. Since the signal mode is described by a linear superposition of just those two modes we know that no photons could fall in any other mode in our decomposition.

We can also provide evidence that it is true by taking an example of a coherent state signal. We use the decomposition of Eq. (7) before taking the expectation value,

$$
\langle\alpha_{\xi_S}|\hat{n}(\xi_S)|\alpha_{\xi_S}\rangle = \langle\gamma\alpha_{\xi_{LO}}|\hat{n}(\xi_{LO})|\gamma\alpha_{\xi_{LO}}\rangle
$$

$$
+ \langle\sqrt{1-|\gamma|^2}\alpha_{\xi_\perp}|\hat{n}(\xi_\perp)|\sqrt{1-|\gamma|^2}\alpha_{\xi_\perp}\rangle \tag{C1}
$$

and

$$
|\alpha|^2 = |\gamma|^2|\alpha|^2 + (1-|\gamma|^2)|\alpha|^2. \tag{C2}
$$

A proof of this fact for any signal state is more subtle, but it begins by introducing an auxiliary mode with no photons in it so that we can treat the change of mode basis thoroughly. This is always allowed since we are extending our single-mode basis to include other modes which have no weight.

We write the signal as $|\pi_S\rangle = |\psi_{\xi_S}\rangle \otimes |0(\xi_{aux})\rangle$. We can now decompose our mode operators in the normal way where $\hat{A}(\xi_S) \rightarrow \gamma\hat{A}(\xi_{LO}) + \sqrt{1-|\gamma|^2}\hat{A}(\xi_S)$, only now we add in the auxiliary mode so we can write the change of basis as the action of a unitary,

$$
\begin{bmatrix} A(\xi_S) \\ A(\xi_{aux}) \end{bmatrix} = \begin{bmatrix} \gamma & \sqrt{1-|\gamma|^2} \\ \sqrt{1-|\gamma|^2} & -\gamma^* \end{bmatrix} \begin{bmatrix} A(\xi_{LO}) \\ A(\xi_\perp) \end{bmatrix}, \tag{C3}
$$

where we have filled in the bottom row by requiring the matrix to be unitary. Now we can calculate $\hat{A}(\xi_S)^\dagger \hat{A}(\xi_S)$ and see that there are terms present that depend on both modes,

$$
\hat{A}^\dagger(\xi_S)\hat{A}(\xi_S) = |\gamma|^2\hat{A}^\dagger(\xi_{LO})\hat{A}(\xi_{LO}) + (1-|\gamma|^2)\hat{A}^\dagger(\xi_\perp)\hat{A}(\xi_\perp)
$$

$$
+ \gamma\sqrt{1-|\gamma|^2}\hat{A}^\dagger(\xi_{LO})\hat{A}(\xi_\perp)
$$

$$
+ \gamma^*\sqrt{1-|\gamma|^2}\hat{A}^\dagger(\xi_\perp)\hat{A}(\xi_{LO}).
$$

Similarly we carry out the same calculation for the auxiliary mode:

$$
\hat{A}(\xi_{aux})^\dagger\hat{A}(\xi_{aux}) = |\gamma|^2\hat{A}(\xi_\perp)^\dagger\hat{A}(\xi_\perp) + (1-|\gamma|^2)\hat{A}(\xi_{LO})^\dagger
$$

$$
\times \hat{A}(\xi_{LO}) - \gamma\sqrt{1-|\gamma|^2}\hat{A}(\xi_{LO})^\dagger\hat{A}(\xi_\perp)
$$

$$
- \gamma^*\sqrt{1-|\gamma|^2}\hat{A}(\xi_\perp)^\dagger\hat{A}(\xi_{LO}).
$$

We now take expectations of the auxiliary mode $\langle\hat{A}(\xi_{aux})^\dagger\hat{A}(\xi_{aux})\rangle = 0$ and we get the following condition:

$$
\langle|\gamma|^2\hat{A}^\dagger(\xi_\perp)\hat{A}(\xi_\perp) + (1-|\gamma|^2)\hat{A}^\dagger(\xi_{LO})\hat{A}(\xi_{LO})\rangle
$$

$$
= \langle\gamma\sqrt{1-|\gamma|^2}\hat{A}^\dagger(\xi_{LO})\hat{A}(\xi_\perp)
$$

$$
+ \gamma^*\sqrt{1-|\gamma|^2}\hat{A}^\dagger(\xi_\perp)\hat{A}(\xi_{LO})\rangle. \tag{C4}
$$

Now we take the expectation in the signal mode,

$$
\langle\hat{A}^\dagger(\xi_S)\hat{A}(\xi_S)\rangle = \langle|\gamma|^2\hat{A}^\dagger(\xi_{LO})\hat{A}(\xi_{LO}) + (1-|\gamma|^2)\hat{A}^\dagger(\xi_\perp)
$$

$$
\times \hat{A}(\xi_\perp)\rangle + \langle\gamma\sqrt{1-|\gamma|^2}\hat{A}^\dagger(\xi_{LO})\hat{A}(\xi_\perp)
$$

$$
+ \gamma^*\sqrt{1-|\gamma|^2}\hat{A}^\dagger(\xi_\perp)\hat{A}(\xi_{LO})\rangle. \tag{C5}
$$

Finally, we just plug in the condition we derived above to get

$$\langle \hat{A}^\dagger(\xi_S)\hat{A}(\xi_S)\rangle = \langle \hat{A}^\dagger(\xi_\perp)\hat{A}(\xi_\perp)\rangle + \langle \hat{A}^\dagger(\xi_{LO})\hat{A}(\xi_{LO})\rangle, \quad \text{(C6)}$$

as desired.

APPENDIX D: COMBINATION RULE FOR POVM

Starting from the total Kraus operator in n and m variables [Eq. (11)],

$$M_{n,m} = \sum_{p,q} M_{p,q}(\xi_{LO}) \otimes M_{n-p,m-q}(\xi_\perp). \quad \text{(D1)}$$

We can rewrite the order of this sum in terms of discrete sum and difference variables,

$$M_{n,m} = \sum_{p+q=0}^{n+m} \sum_{p-q=x_{\min}}^{x_{\max}} M_{p,q}(\xi_{LO}) \otimes M_{n-p,m-q}(\xi_\perp), \quad \text{(D2)}$$

where $x_{\min} = \max(-w, -n, -m)$ and $x_{\max} = -x_{\min}$. This sum can be approximated quite well in the limit where the difference variable is much less than the sum variable,

i.e., $x \ll w$, which is almost always the case for quadrature detection,

$$M_{n,m} = \sum_{p+q=0}^{n+m} \sum_{p-q=-p+q}^{p+q} M_{p,q}(\xi_{LO}) \otimes M_{n-p,m-q}(\xi_\perp). \quad \text{(D3)}$$

Now we move to the sum and difference variables, $x = (p-q)/\sqrt{2}|\beta|$, $w = p + q$. Since we have scaled the difference variable so that it is small, we can approximate the sum over it as an integral. Applying all this in the large-LO limit gives

$$M_{x,w} = \sum_{w'} \int_{-\infty}^{\infty} \frac{|\beta|dx'}{\sqrt{2}} M_{x',w'}(\xi_{LO}) \otimes M_{x-x',w-w'}(\xi_\perp). \quad \text{(D4)}$$

This demonstrates that the total Kraus operator is a convolution of the two constituent Kraus operators. We now need to determine how this convolution changes when we move to the POVMs. This can be done by direct computation but the necessary orthogonality relations are more clear before we move to the sum and difference variables so we will start again from Eq. (11):

$$E_{n,m} = M_{n,m}^\dagger M_{n,m} = \sum_{p,q} M_{p,q}^\dagger(\xi_{LO})M_{n-p,m-q}^\dagger(\xi_\perp) \sum_{p',q'} M_{p',q'}^\dagger(\xi_{LO})M_{n-p',m-q'}^\dagger(\xi_\perp)$$
$$= \sum_{p,q}\sum_{p',q'} M_{p,q}^\dagger(\xi_{LO})(\xi_\perp)M_{p',q'}(\xi_{LO})M_{n-p,m-q}^\dagger M_{n-p',m-q'}(\xi_\perp). \quad \text{(D5)}$$

Now we need to remember the form of the single-mode Kraus operators using Eq. (15),

$$M_{p,q}^\dagger(\xi_{LO})(\xi_\perp)M_{p',q'}(\xi_{LO}) = \langle\beta|U_{BS}^\dagger|p\rangle|q\rangle\langle p|\langle q||q'\rangle|p'\rangle\langle q'|\langle p'|U_{BS}|\beta\rangle = \langle\beta|U_{BS}^\dagger|p\rangle|q\rangle\langle q|\langle p|U_{BS}|\beta\rangle\delta_{p,p'}\delta_{q,q'}, \quad \text{(D6)}$$

where we have applied the orthogonality of Fock states. A similar identity holds for the perpendicular mode. Applying this to the POVM reduces the four sums to a sum over just two variables, so we get

$$E_{n,m} = \sum_{p,q} M_{p,q}^\dagger(\xi_{LO})M_{p,q}(\xi_{LO})M_{n-p,m-q}^\dagger M_{n-p,m-q}(\xi_\perp)$$
$$= \sum_{p,q} E_{p,q}(\xi_{LO})E_{n-p,m-q}(\xi_\perp). \quad \text{(D7)}$$

From here we notice that this matches the form of what we started with in Eq. (D1) so we can assert that the combination rule for the POVMs in terms of the sum and difference variables is

$$E_{x,w} = \sum_{w'} \int_{-\infty}^{\infty} \frac{|\beta|dx'}{\sqrt{2}} E_{x',w'}(\xi_{LO}) \otimes E_{x-x',w-w'}(\xi_\perp). \quad \text{(D8)}$$

APPENDIX E: TIME-DEPENDENT PHOTORECORD

If we now assume that our detector does produce timing information then we can still get the same answer but our measurement operators must change. We still want to average the time-dependent photorecord which will be accomplished by coarse graining over time. First we must make some assumptions about our detector. We will model the detector time

dependence by saying each detection event is contained in a time bin $(t_i, t_i + \Delta t)$. We will also assume that Δt is small with respect to the total detection time T.

With these assumptions, we can write a corrected form of our detector:

$$|n\rangle_D(t_i) = |0\rangle \otimes \ldots \cdots \otimes |0\rangle \otimes |n\rangle \otimes |0\rangle \otimes \ldots \cdots \otimes |0\rangle$$
$$\equiv |n_i\rangle. \quad \text{(E1)}$$

This represents getting n clicks in the ith time bucket. With these, we can write the most general measurement operator for our apparatus as

$$M_{n,m}(t_i, t_j) = \langle n_i|\langle m_j|U_{BS}, \quad \text{(E2)}$$

which corresponds to n clicks on one detector in the ith and m clicks in the other in the jth bucket. Up to this point, our measurement operators are fully time dependent and indeed this analysis could be continued without coarse graining, but the resulting theory is difficult to parse analytically and seems more suited for numerics. For this reason, we will consider the case of the averaged photocurrent, which requires coarse graining over time.

Once we have the measurement operators we can assemble the POVMs. The fully time-dependent POVMs would be

$$E_{n,m}(t_i, t_j) = M_{n,m}^\dagger(t_i, t_j)M_{n,m}(t_i, t_j) \quad \text{(E3)}$$

and the naively coarse-grained POVMs should be

$$
\begin{aligned}
E_{n,m} &= \sum_{i,j} M_{n,m}^\dagger(t_i, t_j) M_{n,m}(t_i, t_j) \\
&= \sum_{i,j} U_{\mathrm{BS}}^\dagger |n_i\rangle |m_j\rangle \langle n_i| \langle m_j| U_{\mathrm{BS}}.
\end{aligned}
\tag{E4}
$$

but this only accounts for the cases were all n and m clicks were in a single time bin. It should also be possible to get, say, $n/2$ clicks in the first bin and $n/2$ in the second bin for a total of n clicks. So we need to add in these terms:

$$
E_{n,m} = \sum_{n_i}^n \sum_{m_j}^m U_{\mathrm{BS}}^\dagger |n_i\rangle |m_j\rangle \langle n_i| \langle m_j| U_{\mathrm{BS}},
\tag{E5}
$$

where $\sum_{n_i}^n$ indicates a sum over all possible values of $n_1, n_2, \ldots$ such that $\sum_i n_i = n$. An illustrative special case is when there are only two detection windows, (t_1, t_2), and we get

$$
\begin{aligned}
E_{n,m} = \sum_p \sum_q U_{\mathrm{BS}}^\dagger (|p\rangle_1 \otimes |n-p\rangle_2)(|q\rangle_1 \otimes |m-q\rangle_2)(\langle p|_1 \\
\otimes \langle n-p|_2)(\langle q|_1 \otimes \langle m-q|_2) U_{\mathrm{BS}}.
\end{aligned}
\tag{E6}
$$

Now we note that POVMs are basis independent; i.e., the measurement statistics are the same regardless of any change of bases we make on the POVMs. So we can conjugate our POVM by some unitary U so that we move to the Gram-Schmidt basis defined in Eq. (2). This is where we will assume that $\Delta t \ll T$ so that our bin basis spans the same set of functions as our Gram-Schmidt basis. Now we have

$$
\begin{aligned}
V^\dagger E_{n,m} V = \sum_p \sum_q U_{\mathrm{BS}}^\dagger (|p_{\xi_{\mathrm{LO}}}\rangle \otimes |n - p_{\xi_\perp}\rangle)(|q_{\xi_{\mathrm{LO}}}\rangle \\
\otimes |m - q_{\xi_\perp}\rangle)(\langle p_{\xi_{\mathrm{LO}}}| \otimes \langle n - p_{\xi_\perp}|)(\langle q_{\xi_{\mathrm{LO}}}| \\
\otimes \langle m - q_{\xi_\perp}|) U_{\mathrm{BS}},
\end{aligned}
\tag{E7}
$$

where V denotes a change of basis from the numbered modes to the Gram-Schmidt basis. The final expression is equivalent to what we had before. Note that here we are able to limit ourselves to the special case of just two modes because we are omitting the trivial modes that complete our basis, but carry zero photons.

APPENDIX F: COHERENT STATE DIFFERENCE VARIABLE DISTRIBUTION CALCULATIONS

Using the total POVM from Eq. (15) we can derive the distribution of the total measurement by taking the expectation of the POVM in the signal state,

$$
\begin{aligned}
P(x) &= \langle \alpha_{\xi_S} | E_x | \alpha_{\xi_S} \rangle \\
&= \int dx' \langle \gamma\alpha | E_{x'}(\xi_{\mathrm{LO}}) | \gamma\alpha \rangle \\
&\quad \times \langle \sqrt{1 - |\gamma|^2}\alpha | E_{x-x'}(\xi_\perp) | \sqrt{1 - |\gamma|^2}\alpha \rangle.
\end{aligned}
$$

This distribution can naturally be decomposed into two parts, and then combined by a convolution.

First, let us consider the component in the local oscillator mode. The probability distribution is given by

$P(x) = \langle \gamma\alpha_{\xi_{\mathrm{LO}}} | E_{x,\xi_{\mathrm{LO}}}^\beta | \gamma\alpha_{\xi_{\mathrm{LO}}} \rangle$, i.e.,

$$
\begin{aligned}
P(x) &= |\langle x|\gamma\alpha\rangle|^2 = \frac{e^{-x^2}}{\sqrt{\pi}} |\langle 0| e^{\sqrt{2}x\hat{a}} e^{-\hat{a}^2/2} |\gamma\alpha\rangle|^2 \\
&= \frac{e^{-x^2}}{\sqrt{\pi}} |e^{-|\gamma\alpha|^2/2} e^{\sqrt{2}\gamma\alpha} e^{-\gamma^2\alpha^2/2}|^2 \\
&= e^{-|\gamma|^2} \frac{e^{-x^2}}{\sqrt{\pi}} e^{2\sqrt{2}\mathrm{Re}(\gamma\alpha)} e^{-\mathrm{Re}(\gamma^2\alpha^2)}.
\end{aligned}
\tag{F1}
$$

Here we should recall our convention that α is real and that the phase is completely contained in the modes and thus in γ. We can introduce the shorthand $\gamma = \gamma_R + i\gamma_I$.

Now we can complete the square to obtain a Gaussian distribution in x that is not mean zero:

$$
-(x^2 - 2\sqrt{2}x\alpha\gamma_R) = -(x - \sqrt{2}\alpha\gamma_R)^2 + 2\alpha^2\gamma_R^2.
\tag{F2}
$$

With this we can rewrite the distribution

$$
P(x) = \frac{e^{-(x-\sqrt{2}\alpha\gamma_R)^2}}{\sqrt{\pi}} \exp[-\alpha^2(|\gamma|^2 + \gamma_R^2 - \gamma_I^2 - 2\gamma_R^2)],
\tag{F3}
$$

where we have used the fact that $\mathrm{Re}(\gamma^2) = \gamma_R^2 - \gamma_I^2$. It can be shown in a couple lines of algebra that $|\gamma|^2 + \gamma_R^2 - \gamma_I^2 - 2\gamma_R^2 = 0$ and so we end up with just a normal distribution in x:

$$
P(x) = \frac{e^{-(x-\sqrt{2}\alpha\gamma_R)^2}}{\sqrt{\pi}}.
\tag{F4}
$$

For the perpendicular mode we start with Eq. (12),

$$
\begin{aligned}
P(x, w)_\perp = \langle \sqrt{1 - |\gamma|^2}\alpha | \sum_w |w_{\xi_\perp}\rangle \langle w_{\xi_\perp}| \mathrm{Bin}\left(\frac{|\beta|x}{\sqrt{2}} \Big| w, \frac{1}{2}, 0\right) | \\
\times \sqrt{1 - |\gamma|^2}\alpha\rangle,
\end{aligned}
\tag{F5}
$$

where we can apply the explicit formula for the shifted binomial distribution. At this point both x and w are discrete so we will need to move to continuous variables after we simplify the expression. After taking expectation in the coherent state, we have

$$
\begin{aligned}
P(x, w)_\perp = \frac{w!}{\left(\frac{|\beta|x}{\sqrt{2}} + \frac{w}{2}\right)! \left(\frac{w}{2} - \frac{|\beta|x}{\sqrt{2}}\right)!} \\
\times \frac{1}{2^w} \frac{((1 - |\gamma|^2)|\alpha|^2)^w e^{-(1-|\gamma|^2)|\alpha|^2}}{w!},
\end{aligned}
\tag{F6}
$$

which is the product of the shifted binomial and the Poisson distribution. We can simplify this into the product of two Poisson distributions as

$$
\begin{aligned}
P(x, w)_\perp = \left(\frac{(1 - |\gamma|^2)|\alpha|^2}{2}\right)^{w/2 - |\beta|x/\sqrt{2}} \frac{e^{-(1-|\gamma|^2)|\alpha|^2/2}}{\left(\frac{w}{2} - \frac{|\beta|x}{\sqrt{2}}\right)!} \\
\times \left(\frac{(1 - |\gamma|^2)|\alpha|^2}{2}\right)^{w/2 + |\beta|x/\sqrt{2}} \frac{e^{-(1-|\gamma|^2)|\alpha|^2/2}}{\left(\frac{w}{2} + \frac{|\beta|x}{\sqrt{2}}\right)!}.
\end{aligned}
\tag{F7}
$$

Now we move to continuous variables by approximating both Poisson distributions as normal, this is valid so long as $(1 - |\gamma|^2)|\alpha|^2$ is large enough for the central limit theorem to apply. Doing this and applying some algebraic simplification yields

$$P(x, w)_\perp \, dx \, dw = \frac{|\beta| \, dx \, dw}{\sqrt{2}\pi(1 - |\gamma|^2)|\alpha|^2}$$
$$\times \exp\left[-\frac{|\beta|^2 x^2}{(1 - |\gamma|^2)|\alpha|^2}\right]$$
$$\times \exp\left[-\frac{(w - (1 - |\gamma|^2)|\alpha|^2)^2}{2(1 - |\gamma|^2)|\alpha|^2}\right], \quad \text{(F8)}$$

which we can marginalize over w to get the difference variable distribution,

$$P(x)_\perp = \frac{|\beta|}{\sqrt{\pi(1 - |\gamma|^2)|\alpha|^2}} \exp\left[-\frac{|\beta|^2 x^2}{(1 - |\gamma|^2)|\alpha|^2}\right]$$
$$= \mathcal{N}\left(x, \mu = 0, \sigma^2 = \frac{|\alpha|^2(1 - |\gamma|^2)}{2|\beta|^2}\right). \quad \text{(F9)}$$

APPENDIX G: FILTERING THEORY

In single-mode homodyne measurement we know that the measurement reduces to a measurement of a quadrature defined by the phase of the LO. As long as the LO is large enough for the LO shot noise to dominate the signal shot noise we can reduce the effective quadrature noise to that of vacuum fluctuations. For the multimode case we show in Eq. (14) that the measurement is a quadrature measurement convolved with additional intensity noise from the measurement of the mismatched portion of the signal. The goal of filtering in this context is to reduce the intensity-like noise present in our time-averaged outcome while not affecting the quadrature measurement at all.

We will first imagine that we have very fast detectors that collect photons in a very small time bin $d\tau$ for each data point. Over the entire detection interval, T, we will assume we have many data points, i.e., $d\tau \ll T$. We will consider the filtering operation as applying some time-dependent set of weights $f(t)$ to the photocurrent, and then averaging over the filtered data. This means that any outcome of our measurement x is given by

$$x = \int_0^T f(t)x(t) \, dt, \quad \text{(G1)}$$

where we can easily replace this integral with a sum if the detector window $d\tau$ is not infinitesimal.

In order to ensure that the operator being measured is $\hat{Q}(\xi_{\text{LO}})$ any filter we apply must be constant over the LO mode. If this is not the case then the measurement will have reduced sensitivity to the portions of the LO mode when $f(t)$ is small. The extreme example of this is when $f(t) = 0$ on some interval (t_0, t_1); clearly since these data points are completely removed from the final measurement outcome our measurement has no sensitivity to the part of the LO mode. So we conclude that the filter must leave the LO mode unchanged so the measurement is maintained, i.e., $f(t)\xi_{\text{LO}}(t) \propto \xi_{\text{LO}}(t)$.

The set of all possible filters $f(t)$ under these restrictions becomes

$$f(t) = \begin{cases} c & \text{if } \xi_{\text{LO}}(t) \neq 0 \\ g(t) & \text{if } \xi_{\text{LO}}(t) = 0, \end{cases} \quad \text{(G2)}$$

where c is some constant. Without loss of generality we will assume that $c = 1$ because any other choice of constant would merely scale the value of all outcomes, leaving the SNR unchanged. The problem is now to find $g(t)$ so that we have the minimum perpendicular-mode noise in our measurement.

At this point we should note that in many cases $\xi_{\text{LO}}(t)$ is never zero. While ultimately this means that there is no filter that will leave the LO mode unchanged, it may still be desirable to find an approximate filter which greatly increases SNR at the cost of a small change in the measurement. For example, if the LO is a Gaussian pulse then five standard deviations away from the mean might be sufficient to approximate $\xi_{\text{LO}}(t) \approx 0$. If we want to ensure that some small fraction p of the total LO-mode photons are excluded by our gate then we have the condition

$$|\xi_{\text{LO}}(t)|^2 < \frac{p}{d\tau}. \quad \text{(G3)}$$

Let us now consider the case where the signal is a coherent state $|\alpha_{\xi_s}\rangle$. Here semiclassical analysis tells us how the mean and variance will change under the proposed filter:

$$\mu \to 2\text{Re}(\alpha\beta^*)\text{Re}\left(\int_0^T f(t)\xi_{\text{LO}}^*(t)\xi_s(t) \, dt\right),$$

$$\sigma^2 \to |\beta|^2 \int_0^T |f(t)|^2|\xi_{\text{LO}}(t)|^2 \, dt + |\alpha|^2 \int_0^T |f(t)|^2|\xi_S(t)|^2 \, dt. \quad \text{(G4)}$$

Now we apply the fact that $f(t)\xi_{\text{LO}}(t) = \xi_{\text{LO}}(t)$ and the convention that β is real to get the simplified mean,

$$\mu = 2|\beta|\text{Re}(\gamma\alpha), \quad \text{(G5)}$$

and the variance,

$$\sigma^2 = |\beta|^2 + |\alpha|^2 \int_0^T |f(t)|^2|\xi_S|^2$$
$$= |\beta|^2 + |\alpha|^2 \int_0^T |f(t)|^2|\gamma\xi_{\text{LO}} + \sqrt{1 - |\gamma|^2}\xi_\perp|^2. \quad \text{(G6)}$$

We can expand the second term (the one proportional to $|\alpha|^2$) to $\int_0^T |f(t)|^2 [|\gamma\xi_{\text{LO}}|^2 + (1 - |\gamma|^2)|\xi_\perp|^2 + \gamma\sqrt{1 - |\gamma|^2}(\xi_{\text{LO}}^*\xi_\perp + \xi_{\text{LO}}\xi_\perp^*)]$, which eventually gives

$$\sigma^2 = |\beta|^2 + |\alpha|^2\left[|\gamma|^2 + (1 - |\gamma|^2)\int_0^T |f(t)|^2|\xi_\perp|^2\right], \quad \text{(G7)}$$

where we have again used that fact that $f\xi_{\text{LO}} = \xi_{\text{LO}}$ and that $\langle\xi_{\text{LO}}, \xi_\perp\rangle = 0$. Finally we can apply the assumption that $|\beta|^2 \gg |\gamma\alpha|^2$ to get

$$\text{SNR} = \frac{\mu^2}{\sigma^2} = \frac{4|\beta|^2\text{Re}(\gamma\alpha)}{|\beta|^2 + \eta_f|\alpha|^2}, \quad \text{(G8)}$$

where $\eta_f = \int_0^T |f(t)|^2|\xi_\perp|^2$.

APPENDIX H: SINGLE-PHOTON DISTRIBUTION

We start the calculation from the input state in Eq. (29),

$$|\psi\rangle_s = \gamma |1_{\xi_{\text{LO}}}\rangle |0_{\xi_\perp}\rangle + \sqrt{1 - |\gamma|^2} |0_{\xi_{\text{LO}}}\rangle |1_{\xi_\perp}\rangle. \tag{H1}$$

Taking expectation of the POVM would produce four terms because the input state is written as two terms:

$$P(x) = dx \int dx' \langle \psi_s | E_{x'}^{\text{LO}}(\xi_{\text{LO}}) \otimes E_{x-x'}^\perp(\xi_\perp) | \psi_s \rangle$$

$$= \int dx' (\gamma^* \langle 1| \langle 0| + \sqrt{1 - |\gamma|^2} \langle 0| \langle 1|) E_{x'}^{\text{LO}} \otimes E_{x-x'}^\perp | (\gamma |1\rangle |0\rangle + \sqrt{1 - |\gamma|^2} |0\rangle |1\rangle), \tag{H2}$$

where we have simplified the mode labels for conciseness. Now we just note that $\langle m_{\xi_\perp} | E^\perp | n_{\xi_\perp} \rangle \propto \delta_{m,n}$ because it is a projection onto Fock states, and so only two terms survive:

$$P(x) = \int dx' |\gamma|^2 \langle 1|E_{x'}^{\text{LO}}|1\rangle \langle 0|E_{x-x'}^\perp|0\rangle + (1 - |\gamma|^2) \langle 0|E_{x'}^{\text{LO}}|0\rangle \langle 1|E_{x-x'}^\perp|1\rangle$$

$$= \int dx' \frac{|\gamma|^2}{2\sqrt{\pi}} e^{-x'^2} H_1^2(x') \text{Bin}\left(\frac{|\beta|(x-x')}{\sqrt{2}} \bigg| 0, \frac{1}{2}, 0\right) + \frac{(1 - |\gamma|^2)}{\sqrt{\pi}} e^{-x'^2} \text{Bin}\left(\frac{|\beta|(x-x')}{\sqrt{2}} \bigg| 1, \frac{1}{2}, 0\right). \tag{H3}$$

Now we are in a regime of very weak signal where we cannot approximate these binomial distributions as normal; instead we will mimic the discrete distribution by restricting the distribution of $(x - x')$ to only discrete values. In this case that can best be done by approximating the binomial as a sum of δ functions:

$$P(x) = \int dx' \frac{|\gamma|^2}{2\sqrt{\pi}} e^{-x'^2} H_1^2(x') \delta(x - x') + \frac{(1 - |\gamma|^2)}{\sqrt{\pi}} e^{-x'^2} \left(\frac{1}{2} \delta\left(x - x' - \frac{1}{\sqrt{2}|\beta|}\right) + \frac{1}{2} \delta\left(x - x' + \frac{1}{\sqrt{2}|\beta|}\right)\right)$$

$$= \frac{|\gamma|^2}{2\sqrt{\pi}} e^{-x^2} H_1^2(x) + \frac{(1 - |\gamma|^2)}{2\sqrt{\pi}} (e^{-(x-1/\sqrt{2}|\beta|)^2} + e^{-(x+1/\sqrt{2}|\beta|)^2})$$

$$= \frac{1}{2\sqrt{\pi}} [4|\gamma|^2 e^{-x^2} x^2 + (1 - |\gamma|^2)(e^{-(x-1/\sqrt{2}|\beta|)^2} + e^{-(x+1/\sqrt{2}|\beta|)^2})]. \tag{H4}$$

This matches with the results in Eq. (31).

APPENDIX I: COMPARISON OF PROPOSED LO-MODE QUADRATURE PROJECTION LIMIT VERSUS FILTERING DEMONSTRATIONS

Here we compare our conjectured heterodyne quantum limit set by quadrature projection noise in the LO mode with filtering demonstrations [20,21]. First we assume a hyperbolic secant squared temporal intensity profile. Omitting the complex phase, since here we are only concerned with the absolute mode overlap,

$$|\xi_S| = \frac{1}{\sqrt{T}}, \qquad |\xi_{\text{LO}}| = \frac{1}{\sqrt{2\tau}} \text{sech}\left(\frac{t}{\tau}\right). \tag{I1}$$

Here τ is the temporal width of the sech function. The squared mode overlap $|\langle \xi_S, \xi_{\text{LO}} \rangle|^2$ is thus

$$|\gamma|^2 = \frac{\pi^2 \tau}{2T}. \tag{I2}$$

The fully general heterodyne SNR—which can be derived from a purely moment-based analysis and makes no assumptions about the relative strength of signal and LO—is

$$\frac{\langle i_S^2 \rangle}{\langle i_N^2 \rangle} = \frac{2\left(\frac{\eta_q e}{h\nu}\right)^2 \frac{P_{\text{LO}}}{n} P_s}{e \frac{\eta_q e}{h\nu} (P_{\text{LO}} + |\gamma|^2 P_s) B}, \tag{I3}$$

where $\langle i_S^2 \rangle$ is the average signal power, $\langle i_N^2 \rangle$ is the quantum noise solely in the temporal mode of the comb local oscillator, η_q is the quantum efficiency of the detector, e is the

fundamental charge, $h\nu$ is the energy per photon, P_{LO} is the total comb power, n is the number of comb teeth, P_s is the CW power, and B is the resolution bandwidth. For transform-limited sech pulses $\tau = \frac{0.315}{1.76\Delta\nu}$.

In Ref. [20], $\nu = 193$ THz, $T = 10$ns, $\Delta\nu = 32$GHz, $\eta_q = 0.76$, $P_{\text{LO}} = 6$ nW, $P_s = 2.8$ mW, $n = 320$, and $B = 170$ kHz. Our predicted standard quantum limit (SQL) SNR is 54.5 dB versus the experimentally realized SNR of 36.9 dB. In Ref. [20], $\nu = 193$ THz, $T = 10$ ns, $\Delta\nu = 12$ GHz, $\eta_q = 0.7$, $P_{\text{LO}} = 1.74$ μW, $P_s = 0.5$ mW, $n = 120$, and $B = 100$ kHz. Our predicted SQL SNR is 78.6 dB versus the experimentally realized SNR of 68.3 dB. Similar SNR figures arise when assuming a Gaussian profile (54.2 and 78.5 dB for Refs. [20] and [21], respectively).

Similarly, we can calculate η_f for this experiment using some assumptions. Given the 60-ps pulse width we can approximate $f(t)$ by moving five standard deviations away from the pulse mean. Since the signal was a CW laser the integral to calculate η_f is simple and we get the following:

$$\eta_f \approx \frac{5\sigma}{T}. \tag{I4}$$

After correctly converting from pulse width to standard deviations of a Gaussian pulse we get $\eta_f = 1.3 \times 10^{-2}$ for Ref. [20]. Along with the other experimental details, this would result in a potential 18.8-dB improvement, slightly less than the 20 dB they achieved. This difference can be explained

simply because they did not apply a filter that we consider. Additionally, if we choose to approximate our cutoff after only three standard deviations we would have had an improvement of 20.8 dB, which better matches their result.

[1] R. Kumar, E. Barrios, A. MacRae, E. Cairns, E. H. Huntington, and A. I. Lvovsky, Versatile wideband balanced detector for quantum optical homodyne tomography, Opt. Commun. **285**, 5259 (2012).

[2] T. Gerrits, S. Glancy, and S. W. Nam, A balanced homodyne detector and local oscillator shaping for measuring optical Schrödinger cat states, Proc. SPIE **8033**, 80330X (2011).

[3] M. Fuwa, S. Takeda, M. Zwierz, H. M. Wiseman, and A. Furusawa, Experimental proof of nonlocal wavefunction collapse for a single particle using homodyne measurements, Nat. Commun. **6**, 6665 (2015).

[4] C. Polycarpou, K. N. Cassemiro, G. Venturi, A. Zavatta, and M. Bellini, Adaptive detection of arbitrarily shaped ultrashort quantum light states, Phys. Rev. Lett. **109**, 053602 (2012).

[5] Z. Qin, A. S. Prasad, T. Brannan, A. MacRae, A. Lezama, and A. I. Lvovsky, Complete temporal characterization of a single photon, Light: Sci. Appl. **4**, e298 (2015).

[6] S. Grandi, A. Zavatta, M. Bellini, and M. G. A. Paris, Experimental quantum tomography of a homodyne detector, New J. Phys. **19**, 053015 (2017).

[7] N. Walker, Quantum theory of multiport optical homodyning, J. Mod. Opt. **34**, 15 (1987).

[8] S. L. Braunstein, Homodyne statistics, Phys. Rev. A **42**, 474 (1990).

[9] K. Banaszek and K. Wódkiewicz, Operational theory of homodyne detection, Phys. Rev. A **55**, 3117 (1997).

[10] T. Tyc and B. C. Sanders, Operational formulation of homodyne detection, J. Phys. A: Math. Gen. **37**, 7341 (2004).

[11] C. W. Helstrom, Detectability of coherent optical signals in a heterodyne receiver, J. Opt. Soc. Am. **57**, 353 (1967).

[12] J. Shapiro, Quantum noise and excess noise in optical homodyne and heterodyne receivers, IEEE J. Quantum Electron. **21**, 237 (1985).

[13] M. Collett, R. Loudon, and C. Gardiner, Quantum theory of optical homodyne and heterodyne detection, J. Mod. Opt. **34**, 881 (1987).

[14] K. J. Blow, R. Loudon, S. J. D. Phoenix, and T. J. Shepherd, Continuum fields in quantum optics, Phys. Rev. A **42**, 4102 (1990).

[15] R. S. Bennink and R. W. Boyd, Improved measurement of multimode squeezed light via an eigenmode approach, Phys. Rev. A **66**, 053815 (2002).

[16] K. Nakamura, Quantum noise and vacuum fluctuations in balanced homodyne detections through ideal multi-mode detectors, Prog. Theor. Exp. Phys. **2021**, 103A01 (2021).

[17] F. Grosshans and P. Grangier, Effective quantum efficiency in the pulsed homodyne detection of a *n*-photon state, Eur. Phys. J. D **14**, 119 (2001).

[18] Z. Ou, *Quantum Optics For Experimentalists* (World Scientific, Singapore, 2017).

[19] Z. Chen, X. Wang, S. Yu, Z. Li, and H. Guo, Continuous-mode quantum key distribution with digital signal processing, npj Quantum Inf. **9**, 28 (2023).

[20] J.-D. Deschênes and J. Genest, Heterodyne beats between a continuous-wave laser and a frequency comb beyond the shot-noise limit of a single comb mode, Phys. Rev. A **87**, 023802 (2013).

[21] J.-D. Deschênes and J. Genest, Chirped pulse heterodyne for optimal beat note detection between a frequency comb and a continuous wave laser, Opt. Express **23**, 9295 (2015).

[22] M. Walsh, P. Guay, and J. Genest, Unlocking a lower shot noise limit in dual-comb interferometry, APL Photonics **8**, 071302 (2023).

[23] S. A. Diddams, K. Vahala, and T. Udem, Optical frequency combs: Coherently uniting the electromagnetic spectrum, Science **369**, eaay3676 (2020).

[24] K. Beloy, M. I. Bodine, T. Bothwell, S. M. Brewer, S. L. Bromley, J.-S. Chen, J.-D. Deschênes, S. A. Diddams, R. J. Fasano, T. M. Fortier, Y. S. Hassan, D. B. Hume, D. Kedar, C. J. Kennedy, I. Khader, A. Koepke, D. R. Leibrandt, H. Leopardi, A. D. Ludlow, W. F. McGrew *et al.*, Frequency ratio measurements at 18-digit accuracy using an optical clock network, Nature (London) **591**, 564 (2021).

[25] E. D. Caldwell, L. C. Sinclair, N. R. Newbury, and J. D. Deschenes, The time-programmable frequency comb and its use in quantum-limited ranging, Nature (London) **610**, 667 (2022).

[26] Q. Shen, J. Y. Guan, J. G. Ren, T. Zeng, L. Hou, M. Li, Y. Cao, J. J. Han, M. Z. Lian, Y. W. Chen, X. X. Peng, S. M. Wang, D. Y. Zhu, X. P. Shi, Z. G. Wang, Y. Li, W. Y. Liu, G. S. Pan, Y. Wang, Z. H. Li *et al.*, Free-space dissemination of time and frequency with 10^{-19} instability over 113 km, Nature (London) **610**, 661 (2022).

[27] I. Coddington, N. Newbury, and W. Swann, Dual-comb spectroscopy, Optica **3**, 414 (2016).

[28] N. Picqué and T. W. Hänsch, Frequency comb spectroscopy, Nat. Photon. **13**, 146 (2019).

[29] Y. Yao, Y. Jiang, H. Yu, Z. Bi, and L. Ma, Optical frequency divider with division uncertainty at the 10^{-21} level, Natl. Sci. Rev. **3**, 463 (2016).

[30] X. Xie, R. Bouchand, D. Nicolodi, M. Giunta, W. Hänsel, M. Lezius, A. Joshi, S. Datta, C. Alexandre, M. Lours, P.-A. Tremblin, G. Santarelli, R. Holzwarth, and Y. Le Coq, Photonic microwave signals with zeptosecond-level absolute timing noise, Nat. Photon. **11**, 44 (2017).

[31] T. Nakamura, J. Davila-Rodriguez, H. Leopardi, J. A. Sherman, T. M. Fortier, X. Xie, J. C. Campbell, W. F. McGrew, X. Zhang, Y. S. Hassan, D. Nicolodi, K. Beloy, A. D. Ludlow, S. A. Diddams, and F. Quinlan, Coherent optical clock down-conversion for microwave frequencies with 10^{-18} instability, Science **368**, 889 (2020).

[32] J. Reichert, R. Holzwarth, T. Udem, and T. W. Hänsch, Measuring the frequency of light with mode-locked lasers, Opt. Commun. **172**, 59 (1999).

[33] F. Quinlan, T. M. Fortier, H. Jiang, A. Hati, C. Nelson, Y. Fu, J. C. Campbell, and S. A. Diddams, Exploiting shot noise

correlations in the photodetection of ultrashort optical pulse trains, Nat. Photon. **7**, 290 (2013).

[34] O. Pinel, P. Jian, R. M. de Araújo, J. Feng, B. Chalopin, C. Fabre, and N. Treps, Generation and characterization of multi-mode quantum frequency combs, Phys. Rev. Lett. **108**, 083601 (2012).

[35] M. Kues, C. Reimer, J. M. Lukens, W. J. Munro, A. M. Weiner, D. J. Moss, and R. Morandotti, Quantum optical microcombs, Nat. Photon. **13**, 170 (2019).

[36] N. Fabre, G. Maltese, F. Appas, S. Felicetti, A. Ketterer, A. Keller, T. Coudreau, F. Baboux, M. I. Amanti, S. Ducci, and P. Milman, Generation of a time-frequency grid state with in-tegrated biphoton frequency combs, Phys. Rev. A **102**, 012607 (2020).

[37] G. Maltese, M. I. Amanti, F. Appas, G. Sinnl, A. Lemaître, P. Milman, F. Baboux, and S. Ducci, Generation and symmetry control of quantum frequency combs, npj Quantum Inf. **6**, 13 (2020).

[38] Z. Yang, M. Jahanbozorgi, D. Jeong, S. Sun, O. Pfister, H. Lee, and X. Yi, A squeezed quantum microcomb on a chip, Nat. Commun. **12**, 4781 (2021).

[39] Y. Cai, J. Roslund, V. Thiel, C. Fabre, and N. Treps, Quan-tum enhanced measurement of an optical frequency comb, npj Quantum Inf. **7**, 82 (2021).

[40] A. Belsley, Quantum-enhanced absorption spectroscopy with bright squeezed frequency combs, Phys. Rev. Lett. **130**, 133602 (2023).

[41] M. A. Guidry, D. M. Lukin, K. Y. Yang, and J. Vučković, Multimode squeezing in soliton crystal microcombs, Optica **10**, 694 (2023).

[42] H. Shi, Z. Chen, S. E. Fraser, M. Yu, Z. Zhang, and Q. Zhuang, Entanglement-enhanced dual-comb spectroscopy, npj Quantum Inf. **9**, 91 (2023).

[43] R. Loudon, *The Quantum Theory of Light*, 3rd ed. (Oxford University Press, Oxford, 2000).

[44] J. Combes and A. P. Lund, Homodyne measurement with a Schrödinger cat state as a local oscillator, Phys. Rev. A **106**, 063706 (2022).

[45] A. Avagyan, Quantum state characterization using mea-surement configurations inspired by homodyne detection, arXiv:2305.19397.

[46] C. H. Oh, A maximum likelihood estimation method for a mixture of shifted binomial distributions, Korean J. Data Inf. Sci. **25**, 255 (2014).

[47] W. Vogel, Homodyne correlation measurements with weak local oscillators, Phys. Rev. A **51**, 4160 (1995).

[48] G. S. Thekkadath, D. S. Phillips, J. F. F. Bulmer, W. R. Clements, A. Eckstein, B. A. Bell, J. Lugani, T. A. W. Wolterink, A. Lita, S. W. Nam, T. Gerrits, C. G. Wade, and I. A. Walmsley, Tuning between photon-number and quadrature measurements with weak-field homodyne detection, Phys. Rev. A **101**, 031801(R) (2020).

[49] S. Olivares, A. Allevi, and M. Bondani, On the role of the local oscillator intensity in optical homodyne-like tomography, Phys. Lett. A **384**, 126354 (2020).

[50] E. Hubenschmid, T. L. M. Guedes, and G. Burkard, Complete positive operator-valued measure description of multichannel quantum electro-optic sampling with monochromatic field modes, Phys. Rev. A **106**, 043713 (2022).